

# Very low surface recombination velocity in n-type c-Si using extrinsic field effect passivation

Ruy S Bonilla<sup>1,a)</sup>, Frederick Woodcock<sup>1</sup>, and Peter R Wilshaw<sup>1</sup>

<sup>1</sup>*Department of Materials, University of Oxford, Parks Rd, OX1 3PH, Oxford, United Kingdom*

In this article, field-effect surface passivation is characterised as either intrinsic or extrinsic, depending on the origin of the charges present in passivation dielectric layers. The surface recombination velocity of float zone, 1Ωcm, n-type silicon was reduced to 0.15 cm/s, the lowest ever observed for a passivating double layer consisting of thermally grown silicon dioxide and PECVD silicon nitride. This result was obtained by enhancing the intrinsic chemical and field-effect passivation of the dielectric layers with uniform, extrinsic field-effect passivation induced by corona discharge. The position and stability of charges, both intrinsic and extrinsic, was characterised and their passivation effect was seen stable for two months with  $SRV < 2\text{cm/s}$ . Finally, the intrinsic and extrinsic components of passivation were analysed independently. Hydrogenation occurring during nitride deposition was seen to reduce the density of interfacial defect states from  $\sim 5 \times 10^{10} \text{ cm}^{-2} \text{ eV}^{-1}$  to  $\sim 5 \times 10^9 \text{ cm}^{-2} \text{ eV}^{-1}$ , providing a decrease in surface recombination velocity by a factor of 2.5. The intrinsic charge in the dielectric double layer provided a decrease by a factor of 4, while the corona discharge extrinsic field-effect passivation provided a further decrease by a factor of 3.

## I. INTRODUCTION

Enormous technological advancements in silicon photovoltaics have taken place over the last twenty years. Crystalline silicon (c-Si) solar cells reaching 25% efficiency are now available in the market.<sup>1</sup> The interdigitated back contact (IBC) configuration is a key cell geometry capable of delivering such high efficiencies, through the reduction of resistive and shading losses at the front surface.<sup>2</sup> In order for the carriers generated near the front surface to be collected, they must diffuse to the rear contact without

---

a) Corresponding author: [sebastian.bonilla@materials.ox.ac.uk](mailto:sebastian.bonilla@materials.ox.ac.uk)

recombining. Consequently, the recombination rates at the front surface and in the bulk are factors critical to solar cell efficiency.

Advances in processing have improved the quality of silicon, and the minority carrier lifetime in the bulk has risen accordingly. On the other hand, interfaces are inherent crystal defects and relatively efficient recombination centres. As a result, the surfaces of a silicon wafer now account for a significant proportion of carrier recombination. The physical and chemical processes applied to reduce surface recombination rates are collectively termed surface passivation, and exploit two principal effects:

Chemical passivation eliminates dangling bonds by introducing species such as hydrogen and oxygen which reduce the density of recombination centres. Field-effect passivation (FEP) uses an electric field to repel carriers away from the surface and prevent them from recombining at active surface defects. It is well accepted that minimum surface recombination is achieved by combining both chemical and field-effect passivation.<sup>3</sup> To a good approximation, surface recombination ( $U_s$ ) can be described as proportional to the product of the chemical component which is dependent on the density of interface traps at the silicon surface ( $D_{it}$ ), and the field-effect component which determines the concentration of minority carriers at the surface ( $p_s$  in n-type and  $n_s$  in p-type):

$$U_s \propto D_{it} \times p_s, (1)$$

The exact relation is not straight forward but it can be obtained following a modelling formalism such as those suggested in references 3,4. The effectiveness of the surface as a recombination site is characterised by the surface recombination velocity (SRV).

Industrial high-efficiency solar cells are often passivated with plasma enhanced chemical vapour deposited silicon nitride (PECVD SiN). In addition to its effective chemical passivation, the layer induces FEP due to intrinsic fixed charges produced in the film during its growth which generate an electric field. The film's thickness and chemistry can be adjusted to tune its anti-reflection and

passivation properties, but industrially deposited films rarely optimise all three. This is because it is very difficult to control the deposition parameters finely enough to maintain good chemical and field effect passivation, while also achieving the optimum refractive index to obtain ideal anti-reflective properties. Here we introduce the concept of “intrinsic” and “extrinsic” FEP. Intrinsic FEP refers to the effect of charges intrinsic to the film which are produced during growth and extrinsic refers to charges added *after* the film’s deposition. The use of extrinsic FEP thus allows more flexibility in the combined optimisation of the optical properties and the chemical and field effect passivation properties of dielectric films on semiconductors. The resulting enhanced passivation has the potential to significantly improve solar cell efficiency.<sup>5</sup>

External deposition of charge (extrinsic FEP) has been previously used to greatly enhance surface passivation.<sup>6</sup> However, very few reports have analysed, separately, the chemical and field-effect components of the passivation, as is done in this work on standard oxide nitride double layer dielectrics. Extrinsic FEP has been used here to produce specimens with  $SRV < 1\text{cm/s}$ , the lowest surface recombination velocities ever achieved on a double layer dielectric on moderately doped silicon. To achieve this corona charging has been used with a particular focus on uniformity of deposition to ensure all areas of the surface have charge density close to the optimum for FEP. Such ultralow surface recombination velocities highlight the potential of extrinsic FEP as a passivation scheme to further improve passivation of silicon solar cells. The location of the external charge has also been investigated, with capacitance-voltage and Kelvin probe measurements used to determine the extent to which the ions permeate into the surface layers.

## II. EXPERIMENTAL DETAILS

Float zone (FZ), 200  $\mu\text{m}$  thick, 1  $\Omega\text{cm}$ , n-type crystalline silicon (c-Si) wafers were used in this study. Wafers were oxidized in a dry dichloroethylene/oxygen atmosphere, in a Centrotherm tube furnace, to a thickness of  $100 \pm 2$  nm, at a temperature of 1050  $^{\circ}\text{C}$ . Wafers were then diced into  $3 \times 3$   $\text{cm}^2$  samples and a second layer of silicon nitride  $\sim 70 \pm 5$  nm was deposited using a PlasmaLab 80+ PECVD system (Oxford Instruments), with silane  $\text{SiH}_4$  and ammonia  $\text{NH}_3$  as precursor gases. The thicknesses and refractive index of the  $\text{SiO}_2$  and  $\text{SiN}_x$  films were measured using reflectance spectrometry on a Filmetrics 205 instrument. Their refractive indices were 1.54 and 2.25 respectively.

A corona discharge apparatus was built and optimised to provide extrinsic and uniform field effect passivation to the specimens described. Charging was performed at room temperature in laboratory conditions using a +12 kV power supply. All charge concentrations here reported are therefore positive. The non-uniformity is defined here as the coefficient of variation of the charge concentration measured across the whole tested area of the sample, i.e. the ratio of the standard deviation to the mean of charge. To ensure uniformity of charge deposition, a point-to-plane corona configuration was developed (FIG. 1.a). Previous work has shown that the corona current at a given point on a plane, angle  $\theta$  to the normal is well-approximated by Warburg's Law:<sup>7,8</sup>

$$J = J_0 \cos^5(\theta), (2)$$

Increasing the distance from the specimen over which the corona is struck reduces the variation in  $\theta$  across the sample, and increases the uniformity of current. On the other hand the distance between the point electrode and the sample plane must be smaller than the distance between the electrode and the grounded case. This ensures that the electric field is not significantly altered by the grounded case, and that the field lines point evenly towards the sample.

Numerical modelling was carried out to estimate the uniformity as a function of the corona distance, to quantify the possible benefit of a new configuration. Results indicated that a distance of 15 cm would give a corona current with a coefficient of variation of 1 % across a 3 x 3 cm<sup>2</sup> sample (FIG. 1.b), and this was used for the following experiments.

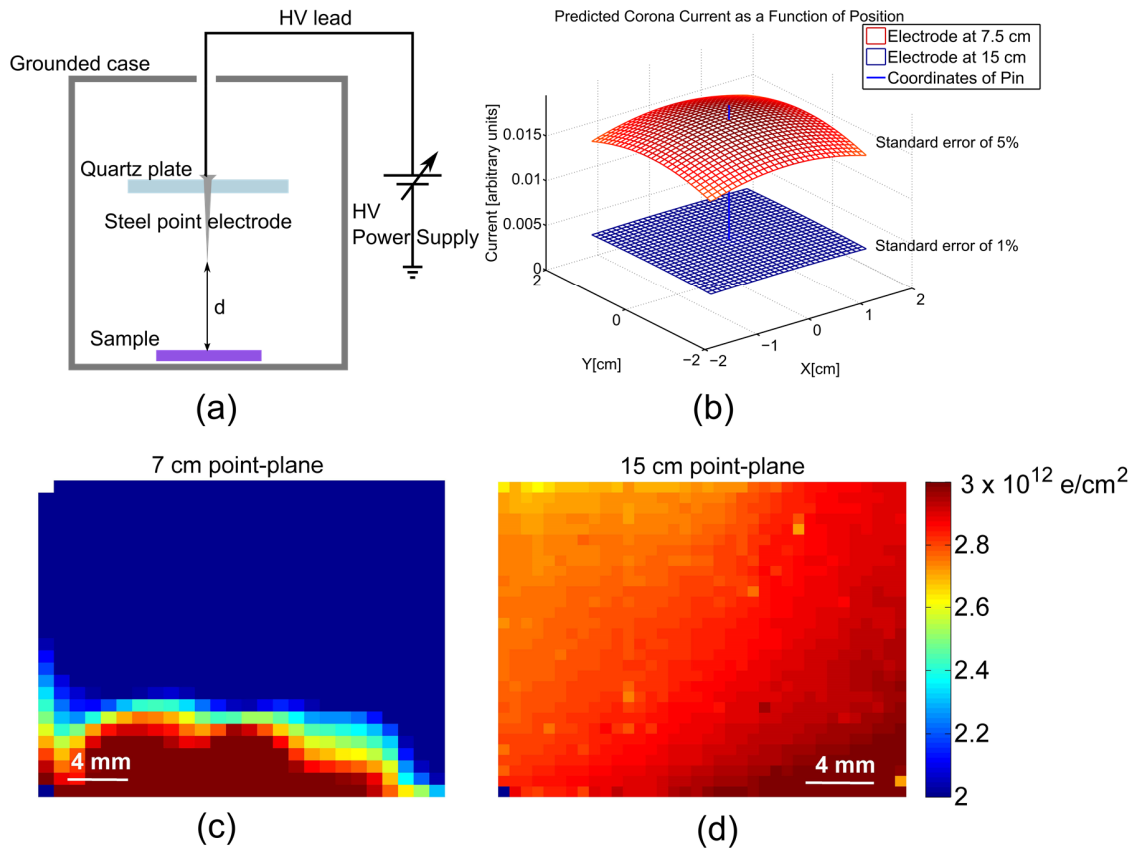


FIG. 1. (a) Circuit diagram of charging apparatus, with corona distance labelled ‘d’. (b) Results of numerical model of Warburg’s Law, showing corona current as a function of position, for corona distances of 7 and 15 cm. (c,d) Kelvin probe charge measurements across positively corona-charged samples with distances 7 and 15 cm. The coefficients of variation were 48% and 4%, respectively

A custom kelvin probe (KP) instrument was used here to estimate charge concentration by measuring surface potential using Baikie’s method.<sup>9</sup> In this set-up the tip was held at ground potential

and the sample was biased to different potentials. Given this configuration, the charge concentration can be estimated from surface potential by solving:<sup>10</sup>

$$V_s = \frac{\Phi_{sm}}{e} - \frac{1}{\epsilon_0} \int_0^{t_i/K_i + t_{air}} x \rho(x) dx - \frac{E_s \epsilon_s}{\epsilon_0 / (t_{air} + t_i/K_i)}, \quad (3)$$

where  $\rho(x)$  is the volume concentration of charge in the dielectric,  $\Phi_{sm}$  is the semiconductor to metal work function difference obtained from a KP measurement on a bare sample,  $K_i$  is the relative permittivity of the dielectric,  $E_s$  is the electric field at the semiconductor surface, and  $t_i/K_i + t_{air}$  represents the distance from the semiconductor/dielectric interface to the tip of the KP, given by the sum of the dielectric thickness plus the air-gap. As will be shown here, the deposited corona charge density ( $\sigma$ ), is generally concentrated in a plane at the insulator-air interface in which case the volume charge distribution is a Dirac delta function centred at the insulator-air interface  $\rho(x) = \sigma \delta(x - t_i/K_i)$ . Given that the distance between the KP tip and the sample is much larger than the electrical thickness of the dielectric ( $t_i/K_i \ll t_{air}$ ), the surface corona charge density can be estimated as:

$$\sigma = \left( \frac{\Phi_{sm}}{e} - V_s \right) \times \epsilon_0 / \left( \frac{t_{ox}}{K_{ox}} + \frac{t_n}{K_n} \right), \quad (4)$$

for a double layer dielectric with electrical thickness  $t/K$ .

The surface charge was mapped using a non-feedbacked XY stage controlled by stepper motors, calibrated to  $\pm 1$  mm accuracy. The maps were constructed on samples that had been charged from 7 and 15 cm (FIG. 1.b,c). In each case, the non-uniformity was higher than the prediction of the model since the samples were not well-centred and the field may be less uniform than the ideal case, but a significant improvement from 48% to 4% was recorded.

A Sinton WCT 120 lifetime tester was used to determine the minority carrier lifetime in samples before and after corona charging, as a function of injection level. Surface recombination velocity has been calculated by subtracting the intrinsic lifetime from effective lifetime, using Richter's

parameterization.<sup>11</sup> The stability of this charge was monitored by taking further measurements as samples aged. Loss of charge can be mediated by water molecules, and it is known that a hydrophobic coating of hexamethyldisilazane (HDMS) increases the stability of charge.<sup>12,13</sup> The samples coated in this work were placed in a furnace with an argon through-flow, and dehydrated at 200°C for 30 minutes. The temperature was then reduced to 120°C, and the argon flow was bubbled through HDMS to coat the surface over a period of 30 minutes.

Test metal-insulator-semiconductor (MIS) specimens were fabricated for high frequency capacitance-voltage (C-V) characterisation. The dielectric layer was removed from the back side by reactive ion etching and a 100 nm layer of aluminium was thermally evaporated thereon. A mercury (Hg) probe with ~0.4 mm radius was used as the front metal contact. A Boonton – 7200 Capacitance Meter was used and capacitance was measured using a 50 mV<sub>pp</sub>, 1 MHz signal. An etch-back experiment was carried out by iteratively etching the silicon nitride layer in an 85 % phosphoric acid (H<sub>3</sub>PO<sub>4</sub>) solution at 160-190 °C, followed by mercury probe C-V measurements to assess charge location in the dielectric. As shown in Section 3, charge present in a nitride/oxide dielectric double layer is found at the interface between the two dielectrics. Gauss' and Green's theorem can be used to demonstrate that, given a surface charge concentration  $\sigma_f$  placed between two insulators:

$$\rho(x) = \sigma_f \delta(x - d_1), \quad (5)$$

with  $x$  running from the metal-dielectric interface to the dielectric-semiconductor one. The shift in the capacitance-voltage relation is given by:<sup>14</sup>

$$\Delta V = \frac{\sigma_f}{\epsilon_0 K_1 / t_1}, \quad (6)$$

where  $d_1 = t_1 / K_1$  is the electrical thickness of the dielectric layer closer to the metal, and  $K_1$  is its electrical permittivity.

### III. RESULTS AND DISCUSSION

The reduction of surface recombination using extrinsic and uniform FEP is shown in FIG. 2. Here, injection-dependent effective lifetime is plotted for 1  $\Omega\text{cm}$  n-type c-Si passivated with different dielectric films. The base film is a forming gas annealed, dry oxide. When this base chemical passivation is subjected to corona charge deposition an improvement in effective lifetime from 0.25 to 3 ms is obtained. This is equivalent to a SRV as low as 2 cm/s at a minority carrier injection of  $10^{15}\text{ cm}^{-3}$ . Such low recombination compares well to that observed using more sophisticated processing –e.g. atomic layer deposited aluminium oxide,<sup>15</sup> amorphous silicon,<sup>16</sup> ‘aneal’ silicon dioxide,<sup>17</sup> and even double layer oxide/nitride films.<sup>18</sup> Given the simplicity of this method, it is important to note that a remarkable surface passivation is available by simply providing extrinsic and uniform FEP. To the best of our knowledge, such level of passivation, achieved primarily by external field-effect, had not been reported before. Other samples were produced using a non-uniform corona rig 7 cm from the sample and maximum lifetimes of  $\sim 2$  ms were achieved. We have consistently seen that the uniformity of the field effect component of passivation is of great importance to produce effective reduction in surface recombination.

Chemical passivation can be additionally improved if a PECVD silicon nitride is deposited on top of the oxide. SiN improves chemical passivation by releasing hydrogen during the deposition process such that many of the interface defect states are effectively eliminated. SiN also contains a moderate intrinsic concentration of charge, as will be described below. When deposited on the base oxide films used here its total effect is a reduction of SRV to  $\sim 3.5$  cm/s. Chemical deposition processes are not perfectly uniform as reported by Veith et al,<sup>15</sup> and consequently charge contained in as-deposited film does not

provide uniform FEP across the full area of a sample. This was also observed by Herasimenka<sup>19</sup> who were able to achieve  $SRV < 1\text{ cm/s}$  on similar material by providing extra FEP by means of corona charge. In the present case a minimum surface recombination velocity has also been obtained by optimizing FEP using extrinsic and uniform corona charge, as shown in FIG. 2 (black solid circles trace). The optimum corona charge concentration was characterized on test specimens using surface potential measurements via Kelvin probe, and was found to be  $\sim 5 \times 10^{12} \text{ e/cm}^2$ . In the best specimen, an effective lifetime of 6.7 ms has been achieved at a minority carrier concentration of  $10^{15} \text{ cm}^{-3}$  for an oxide/nitride layer with such extrinsic and uniform FEP. The SRV for this sample is plotted in the inset of FIG. 2, from which it is evident that SRV can be reduced down to 0.15 cm/s when the chemical and field effect components, both intrinsic and extrinsic, of passivation are jointly and uniformly exploited. To the best of our knowledge, such surface recombination velocity is the lowest seen to date for one or two layer passivation stacks and has only been bettered by that reported by Herasimenka using an a-Si/SiO<sub>2</sub>/SiN<sub>x</sub> three layer stack which was subsequently exposed to corona charge deposition.<sup>19</sup> This very simple technique also outperforms the outstanding passivation achieved by Kerr and Cuevas,<sup>17</sup> which was used to infer the intrinsic lifetime parameterisation most cited for the last decade,<sup>20,21</sup> as shown by the dotted line in FIG. 2. It is clear from FIG. 2 that this parameterisation significantly over estimates the effect of radiative and Auger recombination and hence, for analysis of SRVs in this paper, we use the parameterisation of Richter et al.<sup>11</sup>

The specific contribution of each of the chemical and field effect to overall passivation has been studied using a combination of Kelvin probe and C-V measurements. FIG. 3.a shows typical C-V curves measured on single and double oxide/nitride layers. FIG. 3.b shows the density of interface states obtained using Terman's high frequency C-V method<sup>22</sup> on single oxide and double oxide/nitride layer dielectric films. Prior to nitride deposition the mid-gap value of interface state density ( $D_{it}$ ) is  $\sim 5 \times 10^{10} \text{ cm}^{-2} \text{ eV}^{-1}$ . Terman's method normally under-estimates defect density in comparison to more accurate

methods such as those of Berglund<sup>23</sup> and Castagne.<sup>24</sup> When the nitride is deposited, the density of states is reduced by an order of magnitude to  $\sim 5 \times 10^9 \text{ cm}^{-2} \text{ eV}^{-1}$ . This is typical of the effect silicon nitride deposition has on an oxide/silicon interface. A very important chemical component is therefore observed in the passivation quality of double layers, given by a combination of the already low-defect interface between silicon and silicon dioxide, and the extra hydrogenation that occurs during the PECVD process.

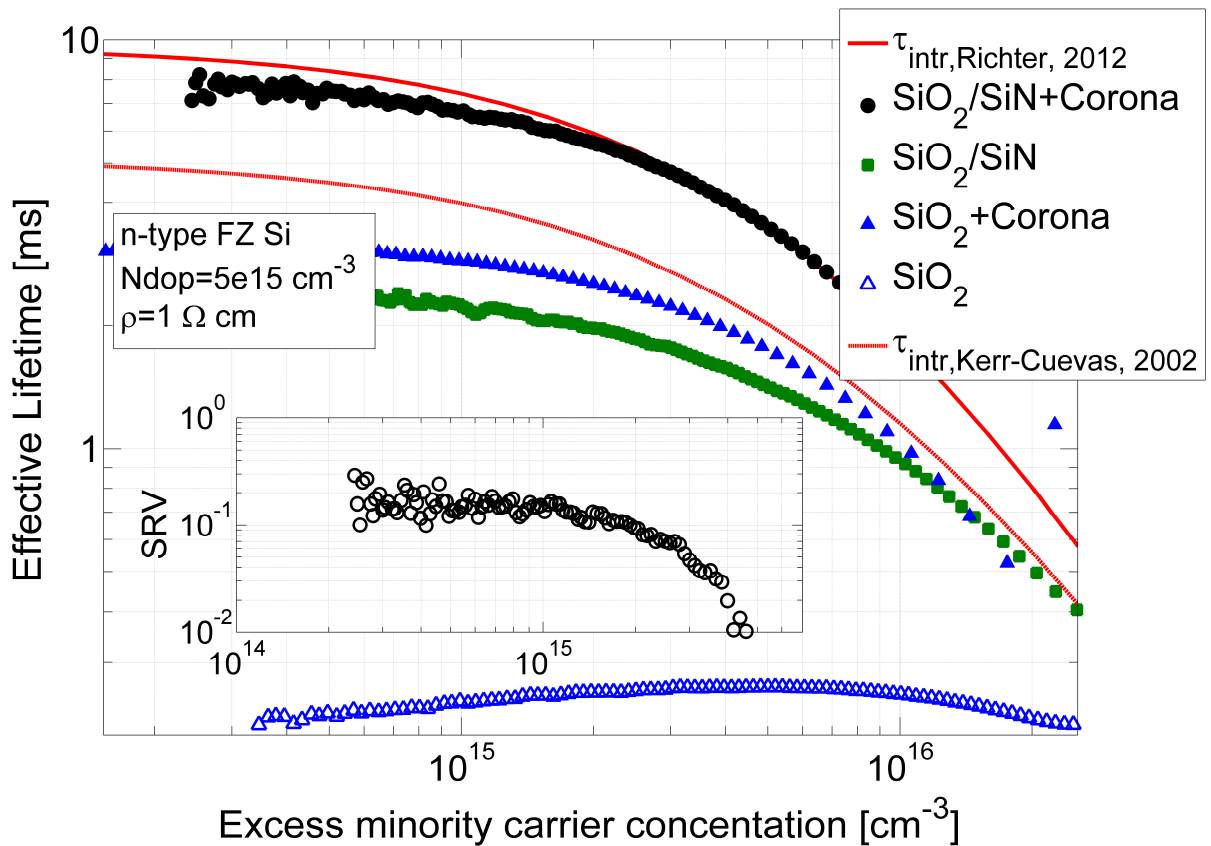


FIG. 2. Injection-dependent effective lifetime for 1Ωcm n-type FZ-Si passivated with a thermally grown oxide and a PECVD deposited nitride, plus the impact of FEP via external corona charge. Inset plots SRV of the SiO<sub>2</sub>/SiN+Corona specimen.

The same specimen in FIG. 3.a was externally deposited with corona charge and measured again using Hg-probe C-V and Kelvin probe. Kelvin probe measurements revealed that the surface charge concentration on this sample was  $\sim 5 \times 10^{12} \text{ e/cm}^2$ , similar to that for specimens in FIG. 2. When

measured via C-V, a small increase in dielectric charge concentration is observed ( $\sim 3 \times 10^{11}$  e/cm<sup>2</sup>), indicating that most of corona-deposited charge is located directly at the nitride-air interface. Gauss' theorem can be used to corroborate this statement, since the shift produced by dielectric charge in C-V measurements is highly dependent on the position of the charge. A complete deduction of the influence of dielectric charge on C-V measurements is given by Snow et al.<sup>25</sup> Superficial charge was subsequently removed from the sample using an isopropyl alcohol (IPA) wash.<sup>26</sup> This was confirmed using KP and C-V measurements. No change in the density of states was observed following this process. Our observations on the location of corona charge and its interaction with the dielectrics disagree with those of Sharma et al.<sup>27</sup> We have not seen corona charge to penetrate the nitride and distribute throughout its thickness. Additionally, we have conducted an etch-back experiment where the nitride has been removed in steps using a phosphoric acid solution (FIG. 3.a inset). This indicates that the charge in an as-deposited nitride/oxide film was located within 20 nm of the interface between the two dielectrics as previously reported,<sup>28</sup> and that all the corona charge was located on top of the nitride, such that it was completely removed with the first etching step, or simply by washing the samples in IPA, as also suggested by other authors.<sup>29,30</sup>

Here, for the first time, we have separated the components of surface passivation (equation 1) over different stages of the processing methodology. PECVD nitride deposition (and the associated H passivation) reduces  $D_{it}$  from  $\sim 5 \times 10^{10}$  to  $\sim 5 \times 10^9$  cm<sup>-2</sup> eV<sup>-1</sup> and provides  $\sim 5-8 \times 10^{11}$  e/cm<sup>2</sup> charge concentration, so reducing SRV from  $\sim 40$  cm/s to  $\sim 3.5$  cm/s. In order to separate the chemical and field-effect components of PECVD silicon nitride passivation we characterized the dielectric charge-SRV relation using a modelling formalism similar to that reported in reference 13. The model included the interface defect density here measured and energy-independent values of hole and electron surface recombination velocities. Using this model the field effect component in the nitride was seen to provide a reduction from  $\sim 40$  cm/s to  $\sim 10$  cm/s. The enhancement of the chemical component by nitride

deposition therefore provides the remaining reduction in SRV, from  $\sim 10$  cm/s to 3.5 cm/s. The final optimization of the passivation scheme used here is that given by extrinsic FEP, which generally further contributes a reduction in SRV by more than a factor of three, from  $\sim 3.5$  cm/s to  $< 1$  cm/s. In the best sample this reduced the SRV to 0.15 cm/s. In summary, when PECVD nitride is deposited on our base oxide films we find surface recombination is reduced by a factor of 10, with the intrinsic FEP accounting for a factor of 4 and the intrinsic chemical a factor of 2.5. Subsequent application of extrinsic FEP further reduces SRV by a factor of  $\gtrsim 3$ .

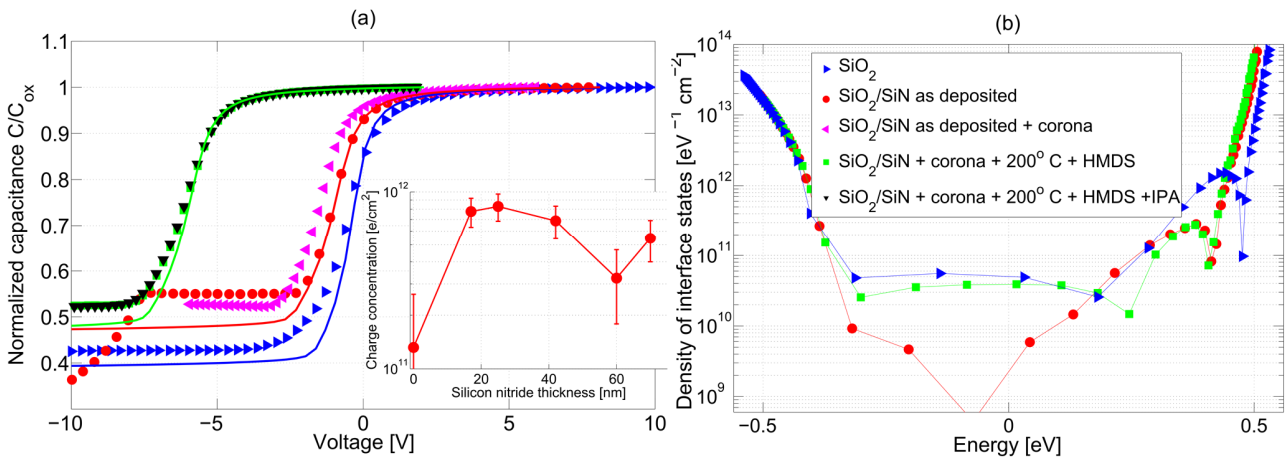


FIG. 3. (a) Capacitance-voltage measurements of single and double layer oxide/nitride films on 1  $\Omega$ cm c-Si. Solid lines represent the ideal theoretical curves. (b) Interface state density calculated for the dielectric layers of (a), using the high frequency C-V Terman's method.

An additional chemical treatment was applied to these samples by dehydration and exposure to HMDS. This step lowered the concentration of charge as checked by a combination of lifetime and KP measurements. Furthermore, some of the deposited corona charge drifted into the film since the Hg-probe C-V measurements afterwards shifted to more negative potentials, as observed in the green square and black down-pointing triangle traces in FIG. 3.a. These charges remained after an IPA wash indicating good stability, however the concentration of defect states at the oxide/semiconductor interface

increased to  $\sim 4 \times 10^{10} \text{ cm}^{-2} \text{ eV}^{-1}$ , thus eliminating the hydrogenation effect achieved via nitride deposition. The location of this charge was assessed via a similar etch-back experiment. Drifted charge was fully removed in the first 10 nm etched of the dielectric, thus indicating that the 200 °C temperature step barely drives the corona charge into the film.

The stability of the processing techniques applied here has been tested over a period of two months. FIG. 4 shows the surface potential and the effective lifetime observed on a corona charged, oxide/nitride double layer passivated specimen. This specimen had an initial effective lifetime of 4.5 ms at an injection level of  $10^{15} \text{ cm}^{-3}$ . Previous reports by the authors<sup>13,31</sup> have demonstrated that once the surface of such film has been chemically treated with a sealant to prevent water absorption, the corona charge is stable for periods exceeding one year. The measurements in FIG. 4 are indicative of this improved stability. A small decay is observed at the start of the measuring period, yet effective lifetimes  $>3$  ms are observed during the remaining two months of measurement. This is equivalent to a SRV  $< 2 \text{ cm/s}$ . A control sample without chemical treatment was also processed and the decay in charge-induced potential is shown in FIG. 4. This is at variance with the report by Sharma et al<sup>27</sup> where samples are claimed stable for a year regardless of the chemical treatment applied to their surfaces.

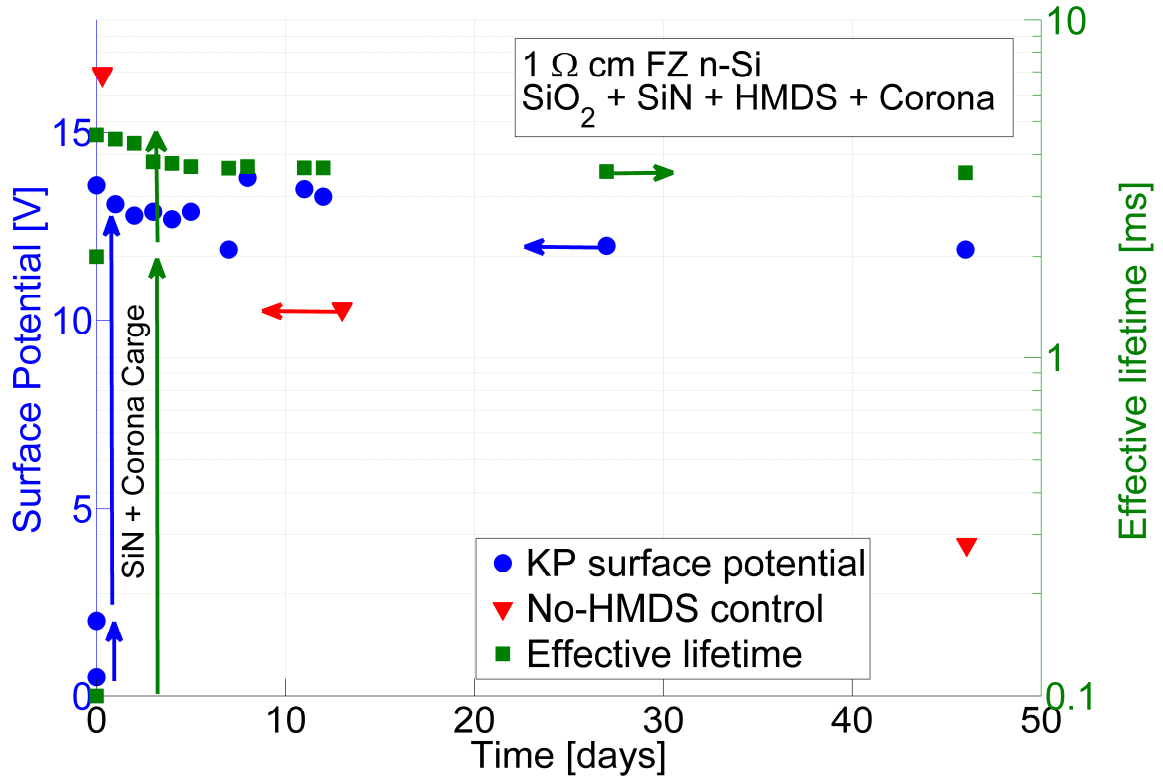


FIG. 4. Long-term stability of extrinsic FEP produced using corona discharge on an oxide/nitride double layer film deposited on 1  $\Omega$ cm c-Si. Measurements on day 0 refer to the processing of the sample given by the nitride deposition and the corona discharge. A control sample lacking chemical treatment is also illustrated.

#### IV. CONCLUSIONS

Remarkable and durable passivation has been shown to be possible by independently combining the best chemical and field effect passivation components of dielectric films produced on silicon. Passivation uniformity has been optimized and it has proven to be a key factor in achieving very low surface recombination velocities. For the first time, a SRV of 0.15 cm/s has been demonstrated on 1 $\Omega$ cm n-Si using an oxide/nitride passivation layer. The stability of extrinsic FEP has been illustrated by maintaining a SRV < 2cm/s. The strong influence of hydrogenation on the silicon surface defect density

was assessed and a one order of magnitude reduction was produced by nitride deposition. The overall contribution of the different components of passivation produced by PECVD deposition of a nitride layer on thermally grown oxide were inferred as follows: the intrinsic FEP due to grown-in charge in the nitride layer accounts for a reduction in recombination by a factor of 4, the improved chemical passivation (due to hydrogen produced during deposition) accounts for a factor of 2.5, and the subsequent addition of extrinsic FEP results in a further factor of 3. The location of charge has been shown to be influential on the passivation quality and stability. These results indicate that controlled and uniform FEP is a key technology to further improve passivation in high efficiency silicon solar cells.

## **ACKNOWLEDGEMENTS**

Ruy S Bonilla is thankful to the Clarendon Fund and Corpus Christi College for providing graduate funding. The authors are thankful to George Martins and Abu Siddique for stimulating discussions, and to Christian Reichel, Martin Hermle, Manuel Schnabel and Stefan Janz at Fraunhofer ISE, for the provision of material.

## **REFERENCES**

<sup>1</sup> P.J. Cousins, D.D. Smith, H.-C. Luan, J. Manning, T.D. Dennis, A. Waldhauer, K.E. Wilson, G. Harley, and W.P. Mulligan, in *2010 35th IEEE Photovolt. Spec. Conf.* (IEEE, 2010), pp. 000275–000278.

<sup>2</sup> M.D. Lammert and R.J. Schwartz, *IEEE Trans. Electron Devices* **24**, 337 (1977).

<sup>3</sup> F.-J. Ma, G.G. Samudra, M. Peters, A.G. Aberle, F. Werner, J. Schmidt, and B. Hoex, *J. Appl. Phys.* **112**, 054508 (2012).

<sup>4</sup> S.W. Glunz, D. Biro, S. Rein, and W. Warta, *J. Appl. Phys.* **86**, 683 (1999).

- <sup>5</sup> A. Rohatgi, P. Doshi, J. Moschner, T. Lauinger, A.G. Aberle, and D.S. Ruby, *IEEE Trans. Electron Devices* **47**, 987 (2000).
- <sup>6</sup> M. Schoffthaler, R. Brendel, G. Langguth, and J.H. Werner, in *Proc. 1994 IEEE 1st World Conf. Photovolt. Energy Convers. - WCPEC (A Jt. Conf. PVSC, PVSEC PSEC)* (IEEE, 1994), pp. 1509–1512.
- <sup>7</sup> E. Warburg, *Handbuch Der Physik, Vol 14* (Springer, Berlin, 1927), pp. 154–155.
- <sup>8</sup> B.L. Henson, *J. Appl. Phys.* **52**, 3921 (1981).
- <sup>9</sup> I.D. Baikie, S. Mackenzie, P.J.Z. Estrup, and J.A. Meyer, *Rev. Sci. Instrum.* **62**, 1326 (1991).
- <sup>10</sup> D.K. Schroder, *Semiconductor Material and Device Characterization* (John Wiley & Sons, Inc., 2006).
- <sup>11</sup> A. Richter, S.W. Glunz, F. Werner, J. Schmidt, and A. Cuevas, *Phys. Rev. B* **86**, 165202 (2012).
- <sup>12</sup> W. Olthuis and P. Bergveld, *IEEE Trans. Electr. Insul.* **27**, 691 (1992).
- <sup>13</sup> R.S. Bonilla and P.R. Wilshaw, in *Energy Procedia - Proc. 3rd Silicon PV Conf.* (Elsevier, Hamelin, Germany, 2013), pp. 816–822.
- <sup>14</sup> R.A. Abbott and T.I. Kamins, *Solid. State. Electron.* **13**, 565 (1970).
- <sup>15</sup> B. Veith, T. Ohrdes, F. Werner, R. Brendel, P. Altermatt, N.-P. Harder, and J. Schmidt, in *Proc. SiliconPV 2013 - Solomat* (n.d.), pp. Hamelin, Germany.
- <sup>16</sup> X. Zhang, S. Hargreaves, Y. Wan, and A. Cuevas, *Phys. Status Solidi - Rapid Res. Lett.* n/a (2013).

- <sup>17</sup> M.J. Kerr and A. Cuevas, *Semicond. Sci. Technol.* **17**, 35 (2002).
- <sup>18</sup> Y. Larionova, V. Mertens, N.-P. Harder, and R. Brendel, *Appl. Phys. Lett.* **96**, 032105 (2010).
- <sup>19</sup> S.Y. Herasimenka, C.J. Tracy, V. Sharma, N. Vulic, W.J. Dauksher, and S.G. Bowden, *Appl. Phys. Lett.* **103**, 183903 (2013).
- <sup>20</sup> J. Schmidt, M. Kerr, and A. Cuevas, *Semicond. Sci. Technol.* **16**, 164 (2001).
- <sup>21</sup> M.J. Kerr and A. Cuevas, *J. Appl. Phys.* **91**, 2473 (2002).
- <sup>22</sup> L.M. and Terman, *Solid. State. Electron.* **5**, 285 (1962).
- <sup>23</sup> C.N. Berglund, *Electron Devices, IEEE Trans.* **13**, 701 (1966).
- <sup>24</sup> R. Castagne and A. Vapaille, *Surf. Sci.* **28**, 157 (1971).
- <sup>25</sup> E.H. Snow, A.S. Grove, B.E. Deal, and C.T. Sah, *J. Appl. Phys.* **36**, 1664 (1965).
- <sup>26</sup> T. Ohmi, S. Sudoh, and H. Mishima, *IEEE Trans. Semicond. Manuf.* **7**, 440 (1994).
- <sup>27</sup> V. Sharma, C. Tracy, D. Schroder, S. Herasimenka, W. Dauksher, and S. Bowden, *Appl. Phys. Lett.* **104**, 053503 (2014).
- <sup>28</sup> R.S. Bonilla, C. Reichel, M. Hermle, and P.R. Wilshaw, *J. Appl. Phys.* **115**, 144105 (2014).
- <sup>29</sup> S. Baker-Finch and K.R. McIntosh, in *3 Rd Int. Sol. Energy Soc. Conf. – Asia Pacific Reg.* (Sydney, Australia, n.d.).
- <sup>30</sup> H. Amjadi, *Dielectr. Electr. Insul. IEEE Trans.* **7**, 222 (2000).

<sup>31</sup> R.S. Bonilla, C. Reichel, M. Hermle, and P.R. Wilshaw, Solid State Phenom. **205-206**, 346 (2013).